Mineralogy and geochemistry of the lithospheric mantle beneath Mir kimberlite pipe, Yakutia: reconstruction for the mantle xenocrysts and xenoliths

M.G., Vavilov (1), I.V. Ashchepkov (1,2),T. Ntaflos (3), A.S. Ivanov (4), I.A., A.M. Logvinova (1), Alymova N.A.(5), N. Medvedev (6)

1 - V.S. Sobolev Institute of Geology and Mineralogy Siberian Branch Russian Academy of Sciences, 630090, Novosibirsk, Koptyuga ave., 3, Russia E-mail: Igora57@mail.ru
2 – NL Dobretsov Institute of Geology, Siberian Branch of the Russian Academy of Sciences, Ulan-Ude, Russia
3. - Vienna University , Austria
4 - Analithic Center, Saint Petersburg Mining University, 21st Line 2, St. Petersburg 199106, Russia
5 - A.P. Vinogradov Institute of Geochemistry SD RAS, Favorsky str. 1A, Irkutsk, 650033, Russia
6 - A.V. Nikolaev Institute of Inorganic Chemistry SB RAS, 630090, Novosibirsk, Acad. Lavrentiev ave, 3, Russia

The geochemical and thermobarometric study of mantle xenoliths and xenocrysts from the Mir kimberlite pipe reveals detailed insights into the pressure-temperature conditions and compositional variations within the mantle section beneath the pipe.

In the mantle column beneath Mir, spans pressures vary from 1.1 to 8 GPa. Mineral thermobarometry shows varying thermal regimes across different pressure intervals. At shallow depths (1.0–3.0 GPa), uneven heating is indicated by ilmenite, chromite, and garnet compositions. Between 3.0 and 4.0 GPa, clinopyroxenes in diamond inclusions show higher temperatures. From 4.5 to 5.0 GPa, garnet and orthopyroxene inclusions align with a relatively cold peridotite geotherm (~800°C), whereas pyroxene inclusions reach up to 1250°C. From 6.0 to 8.0 GPa, chromite data trace an inclined convective geotherm with a temperature gradient about 300°C above the conductive geotherm (35 mW/m²).

Depleted garnets appear from the base of the lithospheric mantle up to 4.5 GPa. CaO content varies significantly in the 5–7.5 GPa interval, dominated by dunites and deformed peridotites. Sub-calcium pyropes in diamond inclusions show increasing Cr_2O_3 with decreasing CaO. Harzburgite garnets and Cr-rich ortho- and clinopyroxenes correspond to cooler geotherms (<35 mW/m²), while Cr-rich diopsides align with slightly higher geotherms (35–40 mW/m²). Peridotites form a reduced branch on the P-fO_2 diagram, being more oxidized upward. Eclogites and ilmenites, along with pyropes from megacrystic associations, indicate more oxidized conditions. Phlogopite and amphibole presence suggests widespread metasomatic influence, especially in the middle to upper mantle sections.

Pyroxenes show variable REE spectra: S-shaped in dunites, semi-circular in lherzolites, and flattened or concave in harzburgites. Pyroxenitic pyropes display a middle-REE (MREE) hump. Eclogite garnets have heavy-REE (HREE) enrichment (~100 times primitive mantle). Most spectra show Th-U peaks; U enrichment is rare in dunites. Small Ta peaks are common; Zr-Hf maxima occur mainly in depleted dunites and garnets. Pb peaks and Ba-Sr minima are typical in garnets; one garnet shows Rb enrichment linked to metasomatism.

The clinopyroxenes (Cpx) from xenocrysts in the Mir kimberlite show highly variable rare earth element (REE) patterns. Most lherzolitic to pyroxenitic Cpx exhibit negatively sloped REE spectra with (La/Yb)_n ratios around 100, featuring small inflection peaks between Sm and Nd. Depleted varieties have gentler slopes, often with a flattened heavy REE (HREE) end and a decrease in light REE (LREE) levels progressing from harzburgites through depleted and garnet-spinel (Gar-Sp) lherzolites. Some pyroxenites and amphiboles, as well as spinel lherzolites with flattened REE spectra, show relatively high HREE concentrations.

Most clinopyroxenes display minor positive anomalies for Th, U, and Pb, along with dips in certain regions. Lithophile element contents are generally low on spider diagrams. Within harzburgite-lherzolite groups, variations in Ta-Nb, as well as contrasting peaks or minima in Ba, Rb, U, Pb, and Sr, are observed. Undepleted varieties tend to have minor Hf-Zr minima, whereas depleted varieties show more pronounced minima with Zr < Hf.

Overall, this study illuminates the complex thermal, compositional, and redox structure of the mantle beneath the Mir kimberlite, with implications for mantle dynamics, metasomatic processes, and diamond formation conditions.

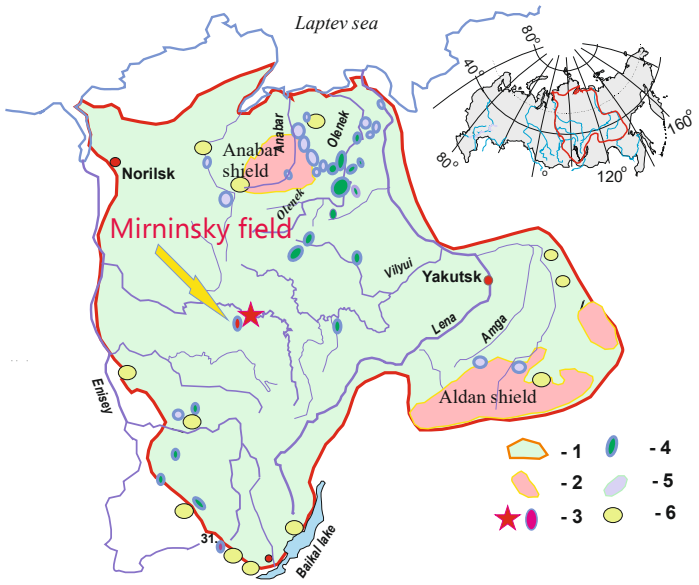

Figure. 1 A The scheme of the Mirninsky field and their position on the Siberian craton. 1. Siberian platform. 2. Precamprian shields. 3. Studied Aalakit -Markha field. 4. Upper Paleozoic kimberlite fields. 5. Mesozoic kimberlite fields. 6. Carbonatite massifs.

Figure 2A. Distribution of the Mir and other kimberlite pipes (1) im Mirninsky field, Siberian craton, cosmic image

The 3D image of Mir pipe (Kostrovitsky, 2025)

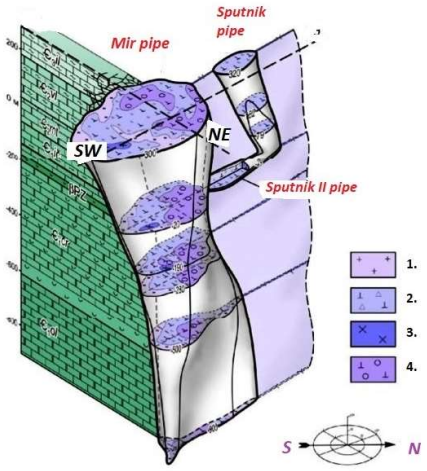

Photo of Mir pipe

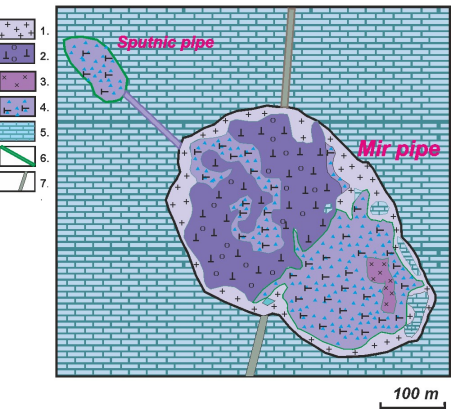

Figure 3. Map and Cross-section of the Mir pipe. (Khar'kiv et al., 1998).

Signs: Kimberlites:

1. Porphyric massive kimberlites, 1st phase.
2. Kimberlite breccias composed of small debr the eastern part of the pipe, phase 2.
3. Autolithic kimberlite breccias of the central part, phase 3.
4. Tuffisitic kimberlite breccias of the eastern part - 4th phase;
5. Kimberlite breccias of the explosive stage, phase 5.

Sedimentary basement: 6. Upper Cambrian, Markha suit – dolomites; 7. Markoka suit- terrigenic carbonate rocks; 8. Lower Ordovician Kylakh suit - cl carbonatic rocks

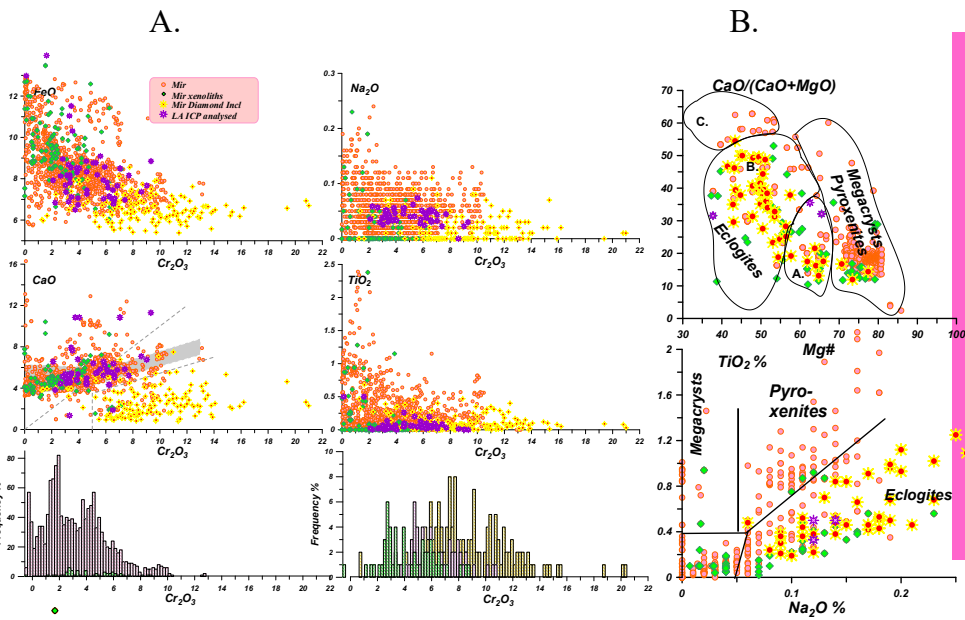

Figure 4. Variation diagrams for garnets from mantle xenoliths from Mir pipe.
A. Variation diagram for the Mg-pyropes. The fields in Cr2O3-CaO plot after Sobolev et al. (1974). 1. Autholithic kimberlite breccia. 2. Tuffisitic kimberlite breccia (Rebus). 3. Diamond inclusions. 4. Samples analyzed by LA ICP MS
B. The variations of garnets on Mg# - CaO/(CaO+MgO) and Na2O-TiO2 diagrams.

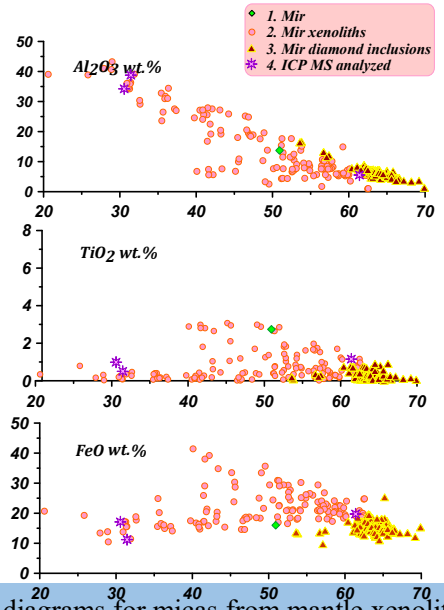

Figure 6. Variation diagrams for chromites from mantle xenoliths from Mir pipe. Symbols the same as for Fig.4

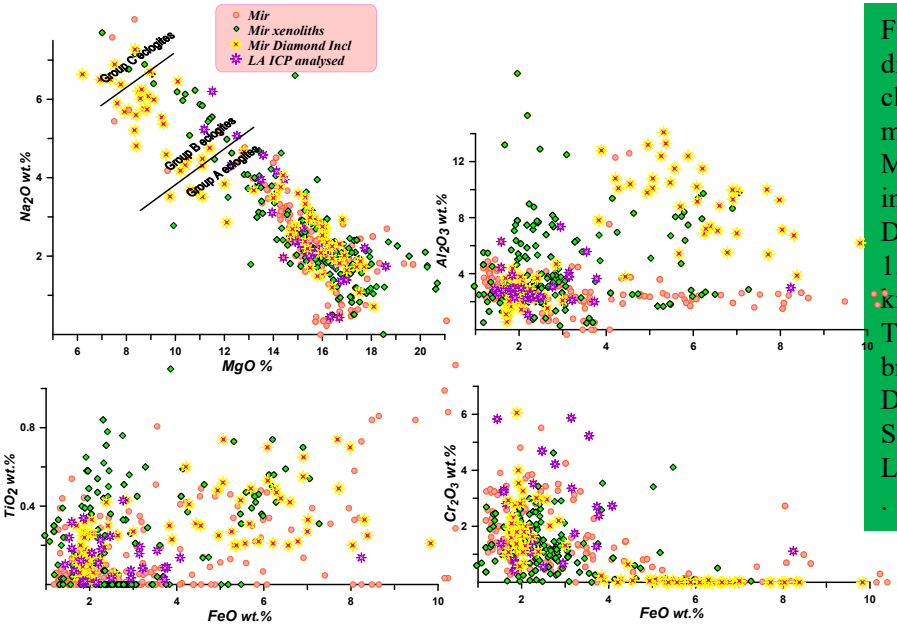

Figure 5. Variation diagrams for clinopyroxenes from mantle xenoliths from Mir pipe. The division in MgO-Na2O after Dawson (1980).
1. Autholitic kimberlite breccia. 2. Tuffisitic kimberlite breccia (Rebus). 3. Diamond inclusions. 4. Samples analyzed by LA ICP MS
.

Figure 7. Variation diagrams for micas from mantle xenoliths and xenocrysts from Ыщкpipe. Division of fields and arrows after Wyatt et al. (2004)ю The lines and arrows are according to (Giulianni et al..2016). Symbols the same as for Fig.4

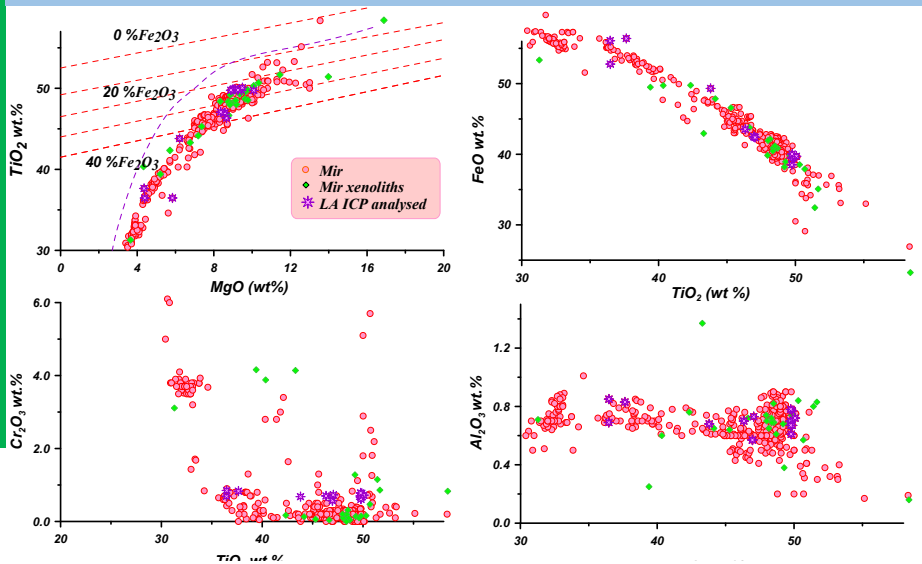

Figure 8. PTXfO_2 diagram for the SCLM beneath the Mir pipe reconstructed with the (A) mantle xenocrysts (B) with xenoliths

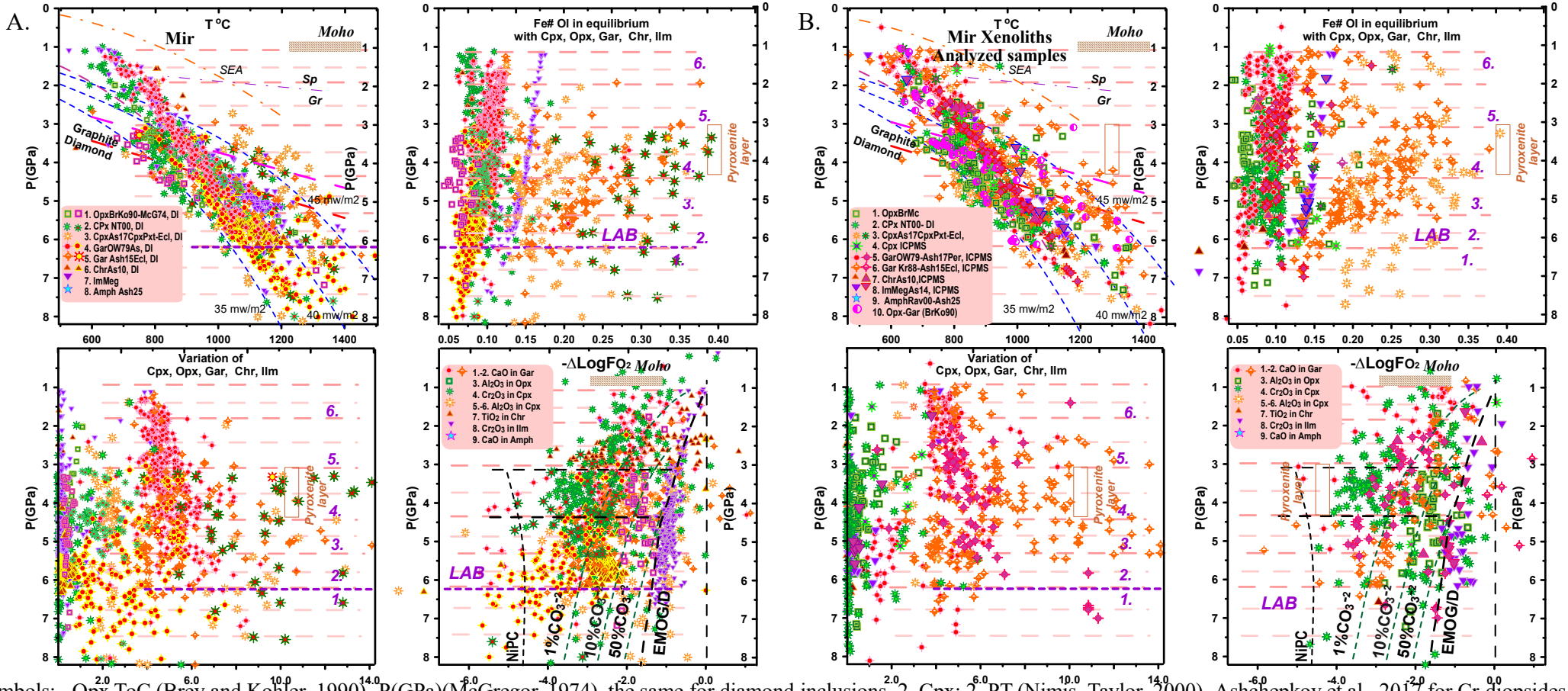

Symbols: . Opx ToC (Brey and Kohler, 1990)- P(GPa)(McGregor, 1974), the same for diamond inclusions. 2. Cpx: 2. PT (Nimis, Taylor, 2000)- Ashchepkov et al., 2017 for Cr-diopsides,), the same for diamond inclusions 3- (Nimis, Taylor, 2000)- Ashchepkov et al., 2017 for pyroxenites and eclogites; 4. Garnets (mono): ToC (O'Neil, Wood, 1979mono)-P(GPa)(Ashchepkov et al., 2010), the same for diamond inclusions ; 5- the same for eclogites and eclogitic diamond inclusions; 6. Chromite: ToC (O'Neil and Wall, 1989)- P(GPa)(Ashchepkov et al., 2010), same for diamond inclusions. 7. Ilmenite ToC (Taylor et al., 1998)- P(GPa) (Ashchepkov et al., 2010).. Amphibole: ToC (Ravna, 2000)- P(GPa) (Ashchepkov, 2017). The oxidation state was calculated using oxybarometers for garnet (Gudmundsson, Wood, 1995), Ilmenites and Cr-Spinelides (Taylor et al., 1998) transformed to monomineral equations according to (Ashchepkov et al., 2010; 2014). The clinopyroxene and orthopyroxene oxybarometers are published in (Ashchepkov et al., 2012a). The isopleth of the CO32- in melt and position of buffers are according to (Stagno et al., 2013). Data for diamond inclusions after (Logvinova et al., 2005). SEA geotherm (O'Reilly and Griffin, 1985). Conductive geotherms after position is after Pollack and Chapman (1977) and the graphite–diamond transition is after Kennedy and Kennedy (1976), revised version of graphite–diamond transition is after Day (2012).

Figure. 10. REE and trace element patterns for garnets from the Mir pipe. A. From lherzolites and pyroxenites. B. From harzburgites. Normalization of REE patterns and spider diagrams to the primitive mantle (McDonough , Sun, 1995)

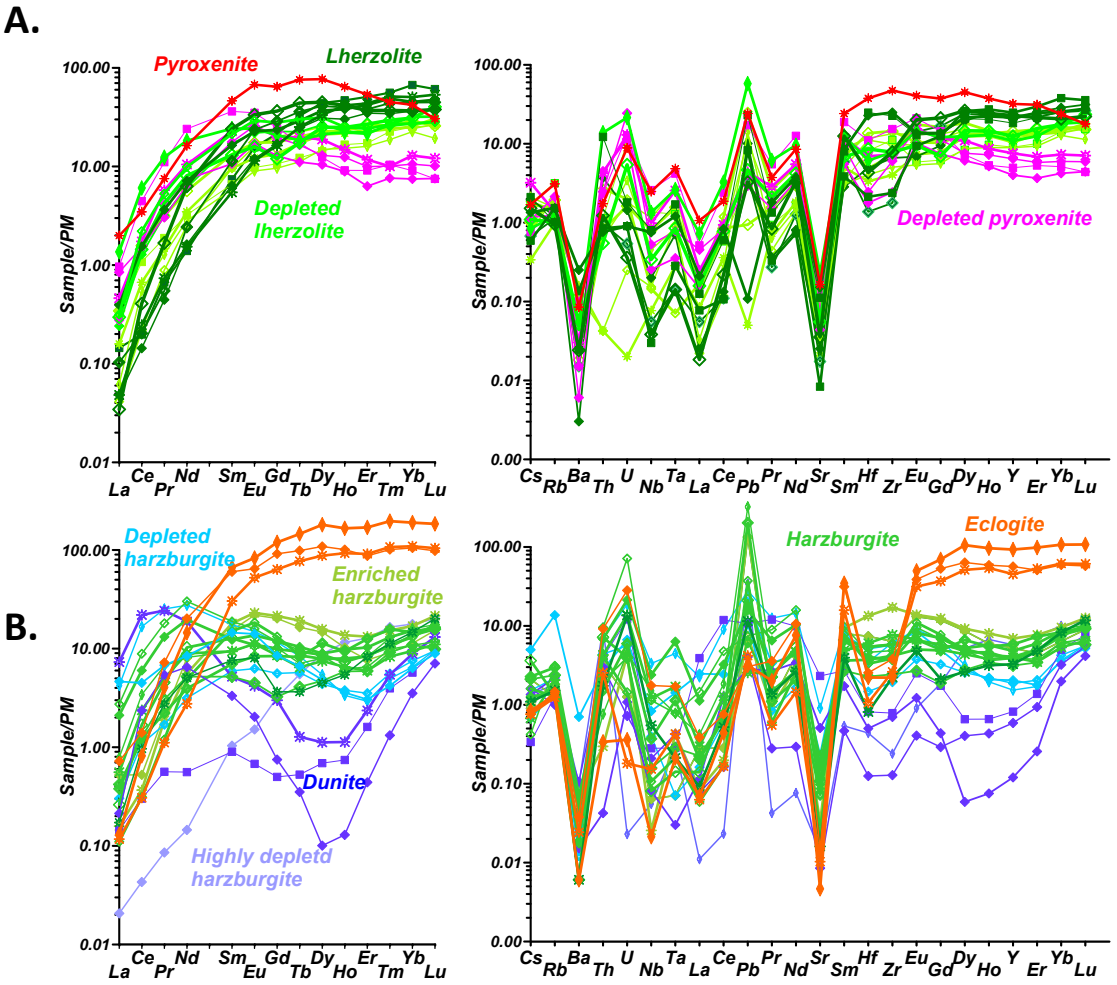

Figure 11. REE and trace element patterns for Clinopyroxenes Mir pipe. Normalization of REE the same

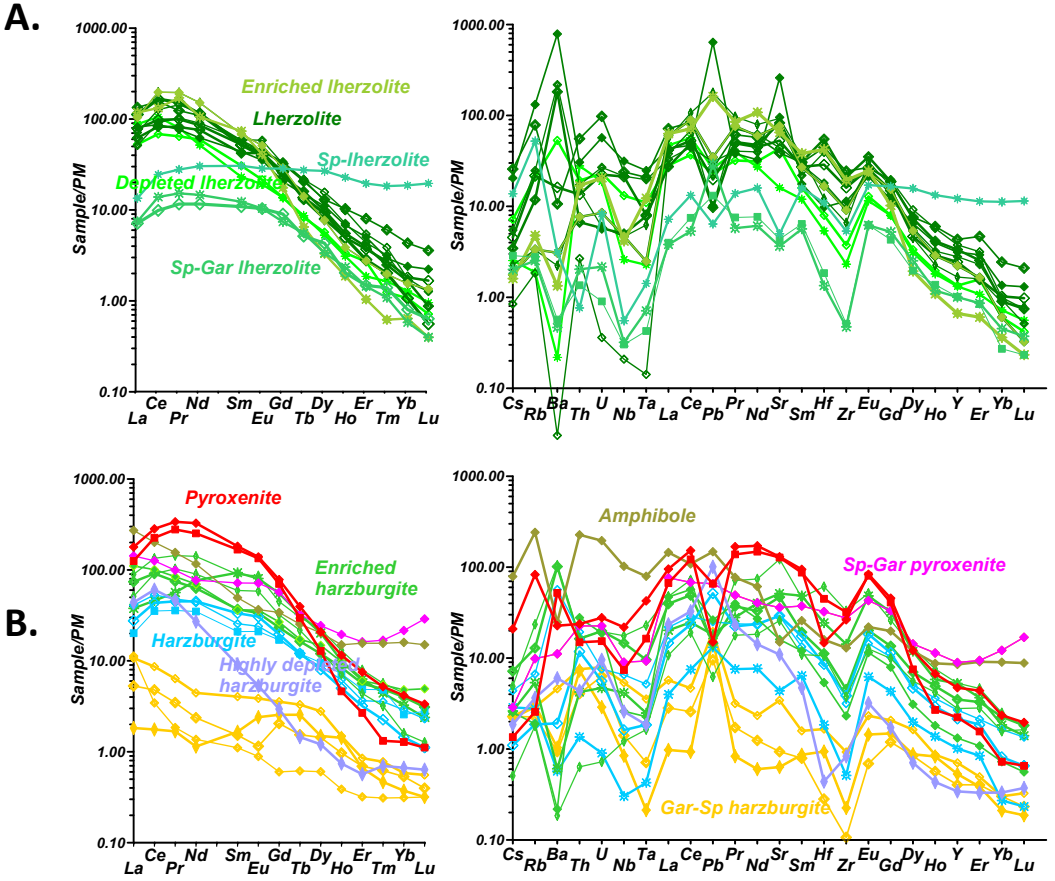

Figure 13. REE and trace element patterns for Ilmenites and chromites from AKB of Mir pipe. Normalization of REE the same

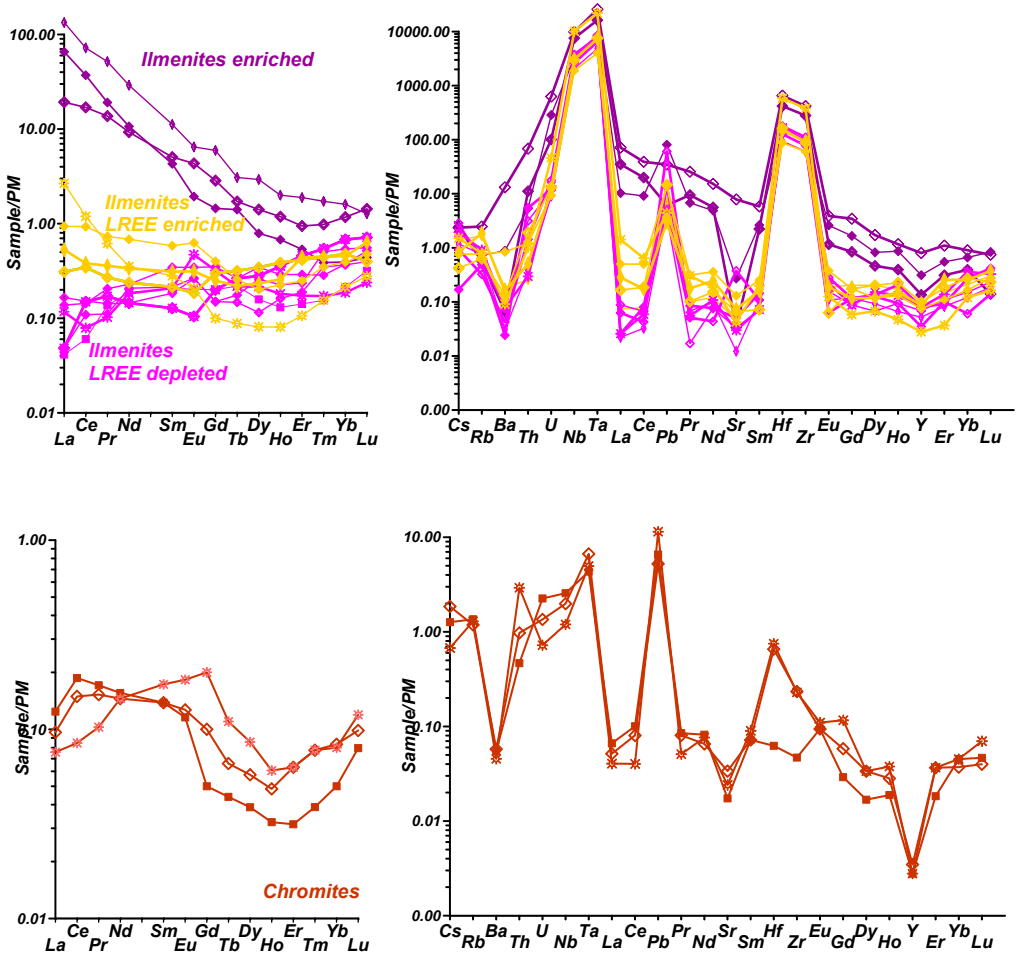

Figure 14. REE and trace element patterns for Diamonds from AKB of the Aykhal pipe. Normalization of REE the same

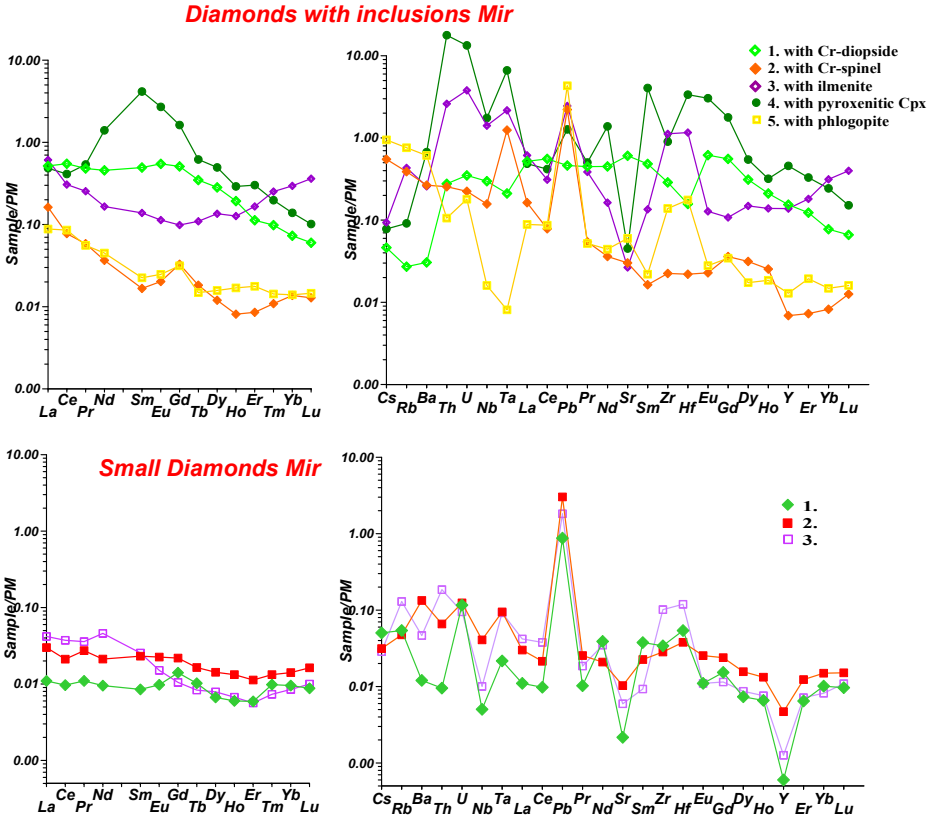

Figure 15. REE and trace element patterns for the melts in equilibrium with the xenocrysts from Mir kimberlitel pipe. Normalization the same

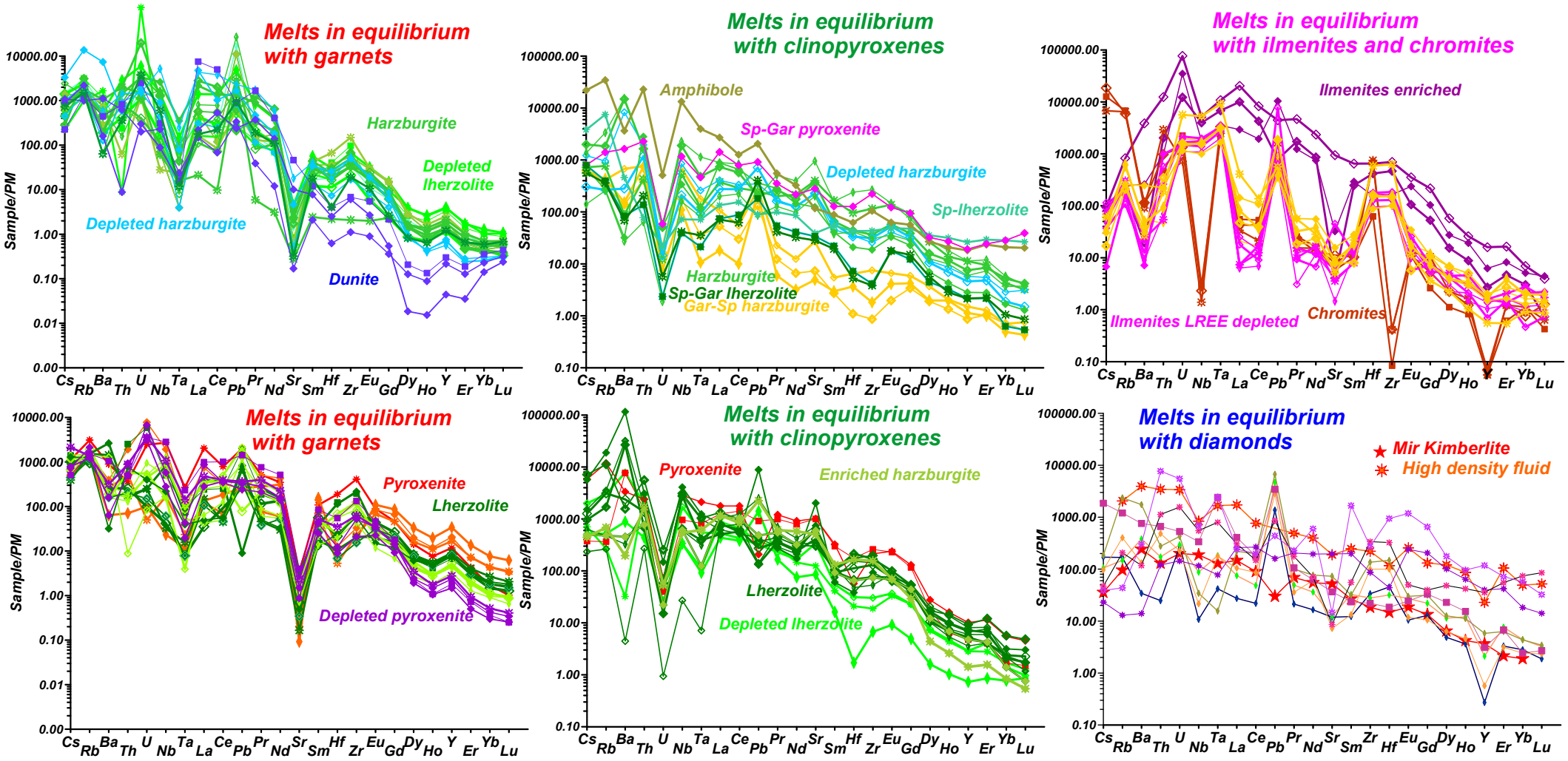

Figure 15. Ternary diagrams for garnets from Mir pipe: A. TiO2-MnO- Na2Ox10 . B., CaO -- TiO2 - Cr2O3 1. Xenocrysts 2. Xenolith. 3. Diamond inclusions

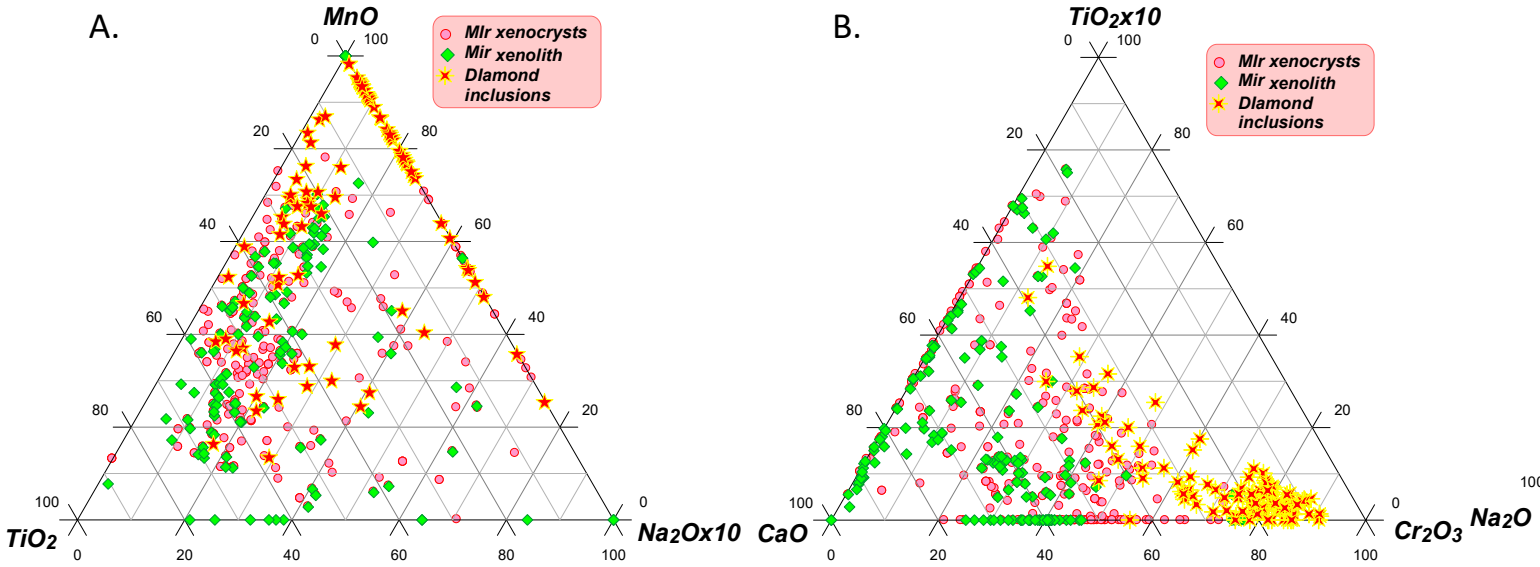

Figure 16. Ternary diagram for clinopyroxenes from Mir pipe: Na2Ox10- TiO2 Cr2O3
1. Xenocrysts 2. Xenolith. 3. Diamond inclusions

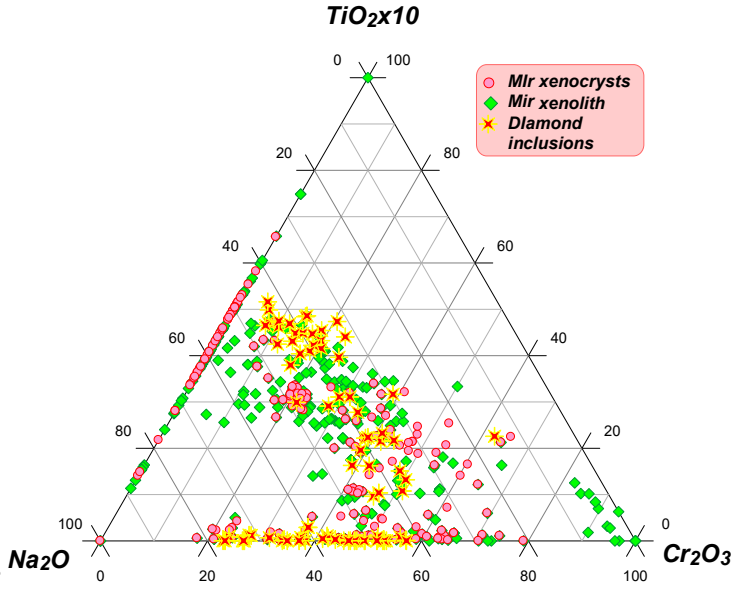

References

Agashev, A. M. (2019, June). Geochemistry of garnet megacrysts from the Mir Kimberlite Pipe (Yakutia) and the nature of protokimberlite melts. In Doklady Earth Sciences (Vol. 486, No. 2, pp. 675-678). Moscow: Pleiades Publishing.

Agashev, A. M., Nakai, S. I., Serov, I. V., Tolstov, A. V., Garanin, K. V., & Kovalchuk, O. E. (2018). Geochemistry and origin of the Mirny field kimberlites, Siberia. Mineralogy and Petrology, 112(Suppl 2), 597-608.

Ashchepkov I.V., Logvinova A.M., Spetsius Z.V., Downes H. 2023. Thermobarometry of diamond inclusions: Mantle structure and evolution beneath Archean cratons and mobile belts worldwide. Geosystems and Geoenvironment 2 (2), 100156. 10.1016/j.geogeo.2022.100156

Ashchepkov, I.V., Alymova, N.V., Logvinova, A.M., Vladykin, N.V., Kuligin, S.S., Mityukhin, S.I., Downes, H., Stegnitsky, Yu.B., Prokopiev, S.A., Salikhov, R.F., Palessky, V.S. Khmel'nikova, O.S., 2014a. Picroilmenites in Yakutian kimberlites: variations and genetic models. Solid Earth 5, 915-938. 10.5194/se-5-915-2014

Ashchepkov, I.V., Ntaflos, T., Logvinova, A.M., Spetsius, Z.V., Downes, H., Vladykin, N.V., 2017a. Monomineral universal clinopyroxene and garnet barometers for peridotitic, eclogitic and basaltic systems. Geoscience Frontiers 8, 775-795. 10.1016/j.gsf.2016.06.012

Ashchepkov, I.V., Logvinova, A.M., Ntaflos, T., Vladykin, N.V., Downes, H., 2017b. Alakit and Daldyn kimberlite fields, Siberia, Russia: Two types of mantle sub-terranes beneath central Yakutia? Geoscience Frontiers 8, 671-692. 10.1016/j.gsf.2014.08.005

Ashchepkov, I.V., Logvinova, A.M., Reimers, L.F., Ntaflos, T., Spetsius, Z.V., Vladykin, N.V., Downes, H., Yudin, D.S., Travin, A.V., Makovchuk, I.V., Palesskiy, V.S., Khmel'nikova, O.S. 2015. The Sytykanskaya kimberlite pipe: Evidence from deep-seated xenoliths and xenocrysts for the evolution of the mantle beneath Alakit, Yakutia, Russia, Geoscience Frontiers, 6(5), 687-714. 10.1016/j.gsf.2014.08.005

Ashchepkov, I.V., Ntaflos, T., Kuligin, S.S., Malygina, E.V., Agashev, A.M., Logvinova, A.M., Mityukhin, S.I., Alymova, N.V., Vladykin, N.V., Palessky, S.V., Khmelnikova, O.S., 2013. Deep-seated xenoliths from the brown breccia of the Udachnaya pipe, Siberia. Pearson et al., eds. Proceedings of 10th International Kimberlite Conference.- New Delhi: Springer India, 1, 59-74. 10.1007/978-81-322-1170-9_5

Ashchepkov, I.V., Ntaflos, T., Spetsius, Z.V., Salikhov, R.F. Downes, H., 2017c. Interaction between protokimberlite melts and mantle lithosphere: Evidence from mantle xenoliths from the Dalnyaya kimberlite pipe, Yakutia , Russia. Geoscience Frontiers 8, 693-710. 10.1016/j.gsf.2016.05.008

Ashchepkov, I.V., Pokhilenko, N.P., Vladykin, N.V., Logvinova, A.M., Kostrovitsky, S.I., Afanasiev, V.P., Pokhilenko, L.N., Kuligin, S.S., Malygina, L.V., Alymova, N.V., Khmelnikova, O.S., Palessky, S.V., Nikolaeva, I.V., Karpenko, M.A., Stagnitsky, Y.B., 2010. Structure and evolution of the lithospheric mantle beneath Siberian craton, thermobarometric study. Tectonophysics 485, 17-41. 10.1016/j.tecto.2009.11.013

Ashchepkov, I.V., Vladykin , N.V., Ntaflos, T., Downes, H., Mitchell, R., Smelov, A.P., Alymova, N.V., Kostrovitsky, S.I., Rotman, A.Ya, Smarov, G.P., Makovchuk, I.V., Stegnitsky, Yu.B., Nigmatulina, E.N., Khmelnikova, O.S., 2013a. Regularities and mechanism of formation of the mantle lithosphere structure beneath the Siberian Craton in comparison with other cratons. Gondwana Research, 23, 4-24. 10.1016/j.gr.2012.03.009

Ashchepkov, I.V., Vladykin, N.V., Nikolaeva, I.V., Palessky, S.V., Logvinova, A.M., Saprykin, A.I., Khmel'nikova, O.S. Anoshin, G.N., 2004. Mineralogy and Geochemistry of Mantle Inclusions and Mantle Column Structure of the Yubileinaya Kimberlite Pipe, Alakit Field, Yakutia. Doklady of RAS ESS 395, 517–523.

Ashchepkov, I. V., Ntaflos, T., Medvedev, N. S., Vladykin, N. V., Logvinova, A. M., Yudin, D. S., Downes, H., Makovchuk, IV., Salikhov, R. F. 2024a. Mantle xenoliths from Komsomolskaya kimberlite pipe, Yakutia: Multistage metasomatism. Geosystems and Geoenvironment, 3(3), 100272. 10.1016/j.geogeo.2024.100272

Ashchepkov, I.V., Ntaflos, N., Medvedev, N.S., Shmarov, G.P. 2024b. Trace element geochemistry of mantle xenoliths from Zarnitsa kimberlite pipe, Daldyn field, Yakutia: complex history of melts interactions with lithospheric mantle Geosystems Geoenvironment, 3 (4), Article 100313. 10.1016/j.geogeo.2024.100313

Ashchepkov, I. V., Vladykin, N. V., Rotman, A. Y., Logvinova, A. M., Afanasiev, V. P., Palessky, V. S., Khmel'nikova, O. S. 2004a. Mir and International'naya kimberlite pipes—trace element geochemistry and thermobarometry of mantle minerals. Deep-seated Magmatism, its Sources and their Relation to Plume Processes. Institute of Geography SB RAS, Irkutsk–Ulan-Ude, 194-208.

Babushkina, S. A., Marshintsev, V. K. 1997. Composition of spinel, ilmenite, garnet, and diopside inclusions in phlogopite macrocrysts from the Mir kimberlite. Russian Geology and Geophysics, 38(2), 467-480.

Beard B.L., Fraracci K.N., Clayton R.A., Mayeda T.K., Snyder G.A., Sobolev N.V., Taylor L.A. 1996. Petrography and geochemistry of eclogites from the Mir kimberlite, Yakutia. Russia Contrib Mineral Petrol 125:293–310. https://doi.org/10.1007/s004100050223

Bobrov, A. V., Sirotkina, E. A., Garanin, V. K., Bovkun, A. V., Korost, D. V., Shkurskii, B. B. 2012. Majoritic garnets with exsolution textures from the Mir kimberlitic pipe (Yakutia). In Doklady Earth Sciences (Vol. 444, No. 1, p. 574). Springer Nature BV. https://doi.org/10.1134/S1028334X12050017

Bulanova, G. P., de Vries, D. W., Pearson, D. G., Beard, A., Mikhail, S., Smelov, A. P., Davies, G. R. 2014. An eclogitic diamond from Mir pipe (Yakutia), recording two growth events from different isotopic sources. Chemical Geology, 381, 40-54. 10.1016/j.chemgeo.2014.05.011

Bulanova, G. P., Pearson, D. G., Hauri, E. H., Griffin, B. J. (2002). Carbon and nitrogen isotope systematics within a sector-growth diamond from the Mir kimberlite, Yakutia. Chemical Geology, 188(1-2), 105-123. https://doi.org/10.1016/j.lithos.2004.04.002

Dymshits, A. M., Sharygin, I. S., Malkovets, V. G., Yakovlev, I. V., Gibsher, A. A., Alifirova, T. A., Vorobei, S.S., Potapov, S.V., Garanin, V. K. 2020. Thermal state, thickness, and composition of the lithospheric mantle beneath the Upper Muna kimberlite field (Siberian craton) constrained by clinopyroxene xenocrysts and comparison with Daldyn and Mirny fields. Minerals, 10(6), 549. doi:10.3390/min10060549

Gubanov, N.V., Zedgenizov, D.A. 2023. The evolution of diamond-forming fluids indicating a pre-kimberlitic metasomatic event in the mantle beneath the Mirny field (Siberian craton). Contrib Mineral Petrol 178, 23. https://doi.org/10.1007/s00410-023-02007-x

Kalashnikova, T. V., Kostrovitsky, S. I., Sinitsyn, K. A., Yudintseva, E. E. 2022. Xenolith Garnets from Mir Kimberlite pipe: chemical composition and evidence of metasomatic processes in the lithosphere mantle. Geodynamics & Tectonophysics, 13 (4) doi:10.5800/gt-2022-13-4-0661

Karputin, I. S., Agashev, A. M., Agasheva, E. V., Serov, I. V., Pokhilenko, N. P. (2025, May). Residual Origin of Garnets and Their Host Lherzolites from the Mir and V. Grib Kimberlite Pipes. In Doklady Earth Sciences (Vol. 522, No. 1, p. 16). Moscow: Pleiades Publishing.

Krot, A. N., Posukhova, T. V., Guseva, Y. V., Galimov, E. M., Botkunov, A. I., Ramenskaya, M. Y., Oglobina, A. I. 1994. Origin of garnets containing hydrocarbon inclusions in the Mir kimberlite pipe. Geochemistry International, 31(1), 122-136.

Novgorodov P.G., Bulanova G.P., Pavlova L.A., Mikhailov V.N., Ugarov V.V., Shebanin A.P., Argunov K.P. 1990. Inclusions of potassic phases, coesite and omphacite in the coated diamond crystal from the '"Mir"' pipe. Dokl Akad Nauk SSSR 310:439–443

Rakhmanova, M. I., Komarovskikh, A. Y., Palyanov, Y. N., Kalinin, A. A., Yuryeva, O. P., & Nadolinny, V. A. (2021). Diamonds from the Mir pipe (Yakutia): spectroscopic features and annealing studies. Crystals, 11(4), 366. doi:10.3390/cryst11040366

Reutskii, V. N., Logvinova, A. M., Sobolev, N. V. (1999). Carbon isotopic composition of polycrystalline diamond aggregates with chromite inclusions from the Mir kimberlite pipe, Yakutia. Geochemistry international, 37(11), 1073-1078.

Roden MF, Patino-Douce AE, Jagoutz E, Laz'ko EE, (2006) High pressure petrogenesis of Mg-rich garnet pyroxenites from Mir kimberlite, Russia. Lithos 90:77–91. https://doi.org/10.1016/j.lithos.2006.01.005

Roden, M. F., Laźko, E. E., Jagoutz, E. 1996. Garnet pyroxenites from the Mir kimberlite pipe; mineral compositions and Sm-Nd systematics of dikes crosscutting coarse garnet lherzolite in the Siberian lithosphere. Eos (Transactions, American Geophysical Union), 77, 277.

Shimizu, N., Sobolev, N.V. 1995. Young peridotitic diamonds from the Mir kimberlite pipe. Nature, 375(6530), 394-397. https://doi.org/10.1038/375394a0

Sirotkina, E. A., Bobrov, A. V., Garanin, V. K., Bovkun, A. V., Shkurskii, B. B., Korost, D. V. (2012, February). Exsolution textures in majoritic garnets from the Mir kimberlite pipe (Yakutia, Russia). In International Kimberlite Conference: Extended Abstracts (Vol. 10).

Skuzovatov, S. Y., Zedgenizov, D. A., Rakevich, A. L., Shatsky, V. S., Martynovich, E. F. 2015. Multiple growth events in diamonds with cloudy microinclusions from the Mir kimberlite pipe: evidence from the systematics of optically active defects. Russian Geology and Geophysics, 56(1-2), 330-343. https://doi.org/10.1016/j.rgg.2015.01.024

Smelova, G. B. (1991, February). Mineral Inclusions in Bort from the Mir Pipe, Yakutia. In International Kimberlite Conference: Extended Abstracts (Vol. 5, pp. 549-550).

Sobolev, N. V., Botkunov, A. I., Kuznetsova, I. K. 1970. A diamond-bearing eciogite with calcium-rich garnet from the" Mir" pipe (Yakutia). International Geology Review, 12(11), 1357-1358.

Sobolev, N. V., Pustyntsev, V. I., Kuznetsova, I. K., Khar'kiv, A. D. 1970. New data on the mineralogy of the diamond-bearing eclogites from the" Mir" pipe (Yakutia). International Geology Review, 12(6), 657-659. Sobolev, N.V, Logvinova, A.M, Zedgenizov, D.A, Seryotkin, Y.V., Yefimova, E.S., Floss, C., Taylor, L.A. 2004. Mineral inclusions in microdiamonds and macrodiamonds from kimberlites of Yakutia: a comparative study. Lithos 77, 225–242.

Sobolev, N.V., Botkunov, A.I., Lavrent'ev, Y.G., Usova, L.V 1976. New data on the minerals associated with the diamonds in the "Mir" kimberlite pipe in Yakutia. Sov. Geol. Geophys., 17, 1–10.

Sobolev, V. N., Taylor, L. A., Snyder, G. A., Sobolev, N. V., Pokhilenko, N. P., Kharkiv, A. D. 1997. A unique metasomatized peridotite xenolith from the Mir kimberlite, Siberian Platform. Russian Geology and Geophysics, 38(1), 218-228.

Spetsius Z.V., Belousova E.A., Griffin W.L., O'Reilly S.Y., Pearson N.J. 2002. Archean sulfide inclusions in Paleozoic zircon megacrysts from the Mir kimberlite, Yakutia: Implications for the dating of diamonds. Earth Planet Sci Lett 199:111–126.

Yuryeva, O. P., Rakhmanova, M. I., Zedgenizov, D. A. 2017. Nature of type IaB diamonds from the Mir kimberlite pipe (Yakutia): evidence from spectroscopic observation. Physics and Chemistry of Minerals, 44(9), 655-667.

Acknowledgements

Work is the supported by the Ministry of Science and Higher Education of the Russian Federation and Russian Science Foundation and partially by Russian Science Foundation (24-27-00411.

Work was done on state assignments of IGM SB RAS FWZN-2026-0007 and Institute of Geochemistry SB RAS, Irkutsk. The authors would like to thank the staff of the analytical services of IGM SB RAS.

Thank you for attention !

The ages of zircon from granulitic xenoliths of Cenozoic volcanics from TransBaikal and Mongolia

AA Tsygankov (1), I.V. Ashchepkov (1,2), G.N. Burmakina

1 – NL Dobretsov Institute of Geology, Siberian Branch of the Russian Academy of Sciences, Ulan-Ude, Russia
2 - V.S. Sobolev Institute of Geology and Mineralogy Siberian Branch Russian Academy of Sciences, 630090, Novosibirsk, Koptyuga ave., 3, Russia E-mail: Igora57@mail.ru
3. - Vienna University , Austria

The ages for zircons from xenoliths of Cenozoic volcanics from TransBaikalia and Mongolia were determined by the same (LA-ICP-MS) aniCAP Q mass spectrometer (Thermo Scientific) and a NWR 213 in IGM SB RAS

The isotopic Pb/U and Pb/Pb ages of the 6 zircon grains from the tuffs of the Bartoy volcano. They are plotting practically on the207Pb/235U and 206Pb/238U concordia line (Figure 9). For the calculations ages the polynomial equations were used obtained from the works of Khubanov et al., (2016-2024).

They may be divided into three groups. The ages of the zircons from tuffs 1160-1250 Ma mainly correspond to the meta-terrigenous rocks of the Shubutuiskaya Formation in the Khamar Daban zone (Gordienko et al., 2006). The Th/U ratio of 0.8-0.6 of these zircons corresponds to the common magmatic rocks, mainly of the basic type (Hawkesworth et al., 1997).

The ages near 800-860 Ma are determined for the suit from the metamorphic in Central Khamar-Daban (Shkol'nik et al., 2016). The collision events at the boundaries of the Paleoasian ocean occurred earlier in the Vend-Cambrian (Byzov, Sankov, 2024; Donskaya et al., 2013). Though some plutons with the model ages 1100-800 Ma were suggested by some authors to be referred to as collision. And elevated Th/U ratios of two zircons, 1.6-1.1, commonly correspond to the granites with the admixture of material of island arc environment with 3-5 Th/U ratios.

The age of granitic zircon, 300 Ma, just corresponds to the beginning of the Angaro-Vitim Batholith (AVP) formation (Tsygankov et al., 2010-2025). It may be connected to the movement of the superplume-formed kimberlites in Yakutia at the interval 420-340 Ma and later created the Biryusa and Tumanshet lamproites (Kostrovitsky et al., 2025) and later the Ingashi lamproites in Eastern Sayan ~306-309 Ma (Gladkochub et al., 2013). Further movement through Khamar-Daban and interaction with the lower crust and granulites brings to the creation of alkaline granitoids of AVP. But the Th/U ratio is rather low, 0.07, which commonly corresponds to the metamorphic type [90]; thus, they should be from granulites possibly remelted by a plume.

The ages from the granulite xenoliths of Vitim picrobasalts (Ashchepkov et al., 2011) corresponds to initial stage of AVB. And the next one 873 may be correlated with the basic magmatism in Baikal uplift (Gladkochub et al., 2010).

In Shavaryn-Tsaram volcano two ages of zircons corresponds to Carboniferous stage 322 Ma of rifting in Mongolia (Kozlovsky et al., 2005) or close to last stage AVP. The next one refers to the initial stage of Miocene plume magmatism (Ashchepkov et al., 2026).

The trace elements for two zircons determined in the granulites highly differ. The inclined enriched in HREE pattern looks similar to carbonatitic zircons (Hardman, et al., 2025). The next acid sample with La/Ybn <2 with Eu minimum and without Ce anomaly. In MSD it shows the same peaks but without Y, Ta anomalies.

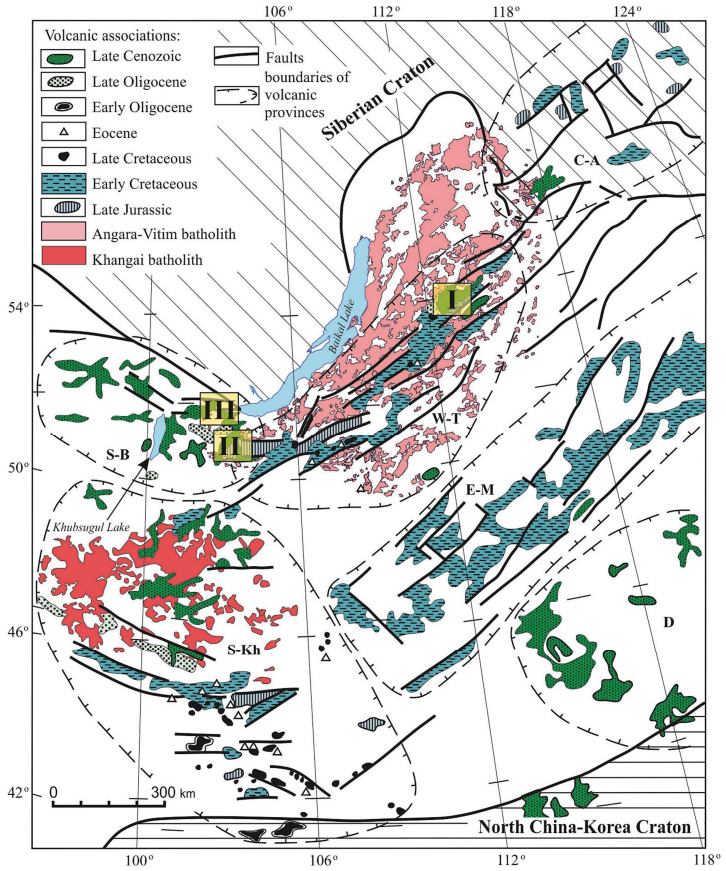

Fig. 1. Distribution scheme of Late Mesozoic-Cenozoic intraplate volcanic rock and Late Paleozoic granitoids in the Central Asia, compiled from (Yarmolyuk et al., 1995) with additions by the authors (a). Volcanic provinces: C-A - Central Aldan, W-T - West Transbaikal, Ssingle bondB - South Baikal, S-Kh - South Khangai, E-M - East Mongolian, D – Dariganga. Roman numerals in circles indicate work areas: I – Vitim Lava Plateau (West Transbaikal volcanic area), II – South Khamar-Daban, Bartoy volcanic group, III – Eastern flank of the Tunka Valley, Karyerny volcano (South Baikal volcanic area). (b) Panorama of the Vitim lava plateau; (c) Quarry on the Kandidushka volcano (Vitim plateau); (d) mantle xenolith (spinel lherzolite); (e) crustal xenolith (mafic granulite).

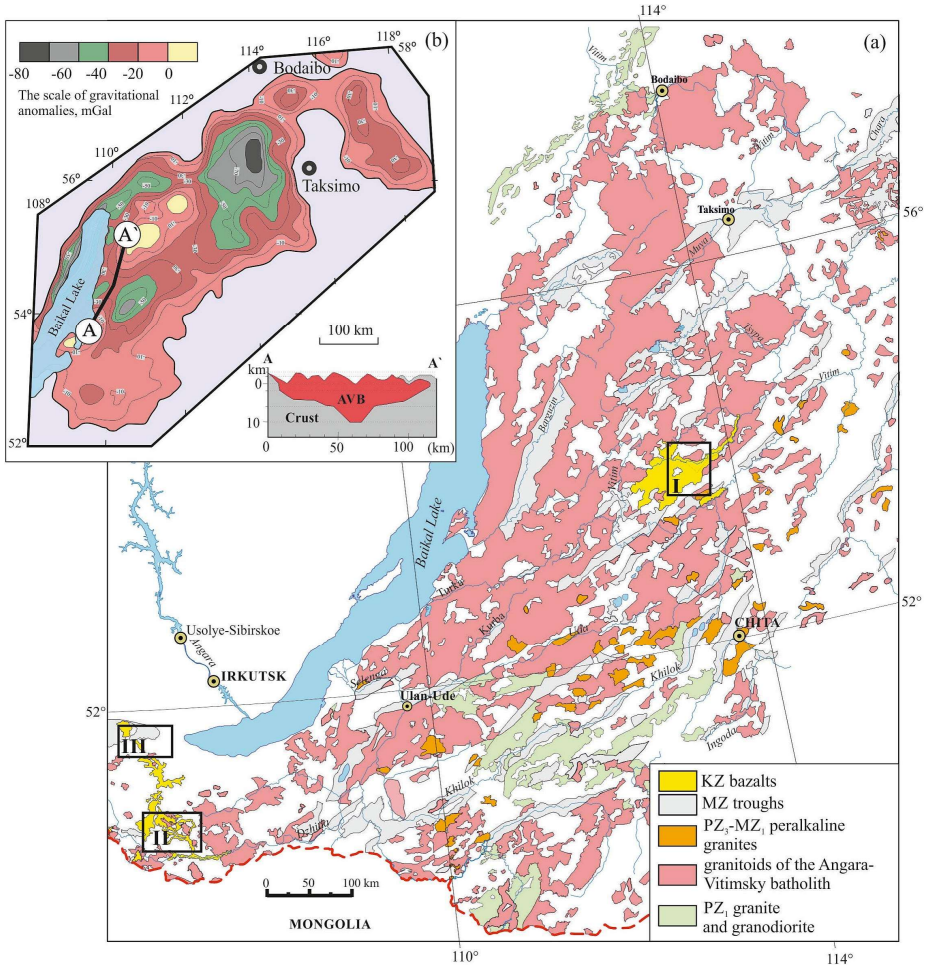

Fig. 2. Distribution scheme of Late Paleozoic granitoids in Western Transbaikalia (a), compiled on the basis of the State Geological Map at a scale of 1:5,000,000; (b) scheme of gravity anomalies (Turutanov, 2011), isolines are drawn through 10 mGal and an interpretation section along line A-A'. Work areas (Roman numerals) correspond to Fig. 1.

Fig.3 Compositions of xenoliths from volcanics of TransKhamarDaban volcanic zone and Bartoy volcanoes (Ashchepkov et al., 2026)

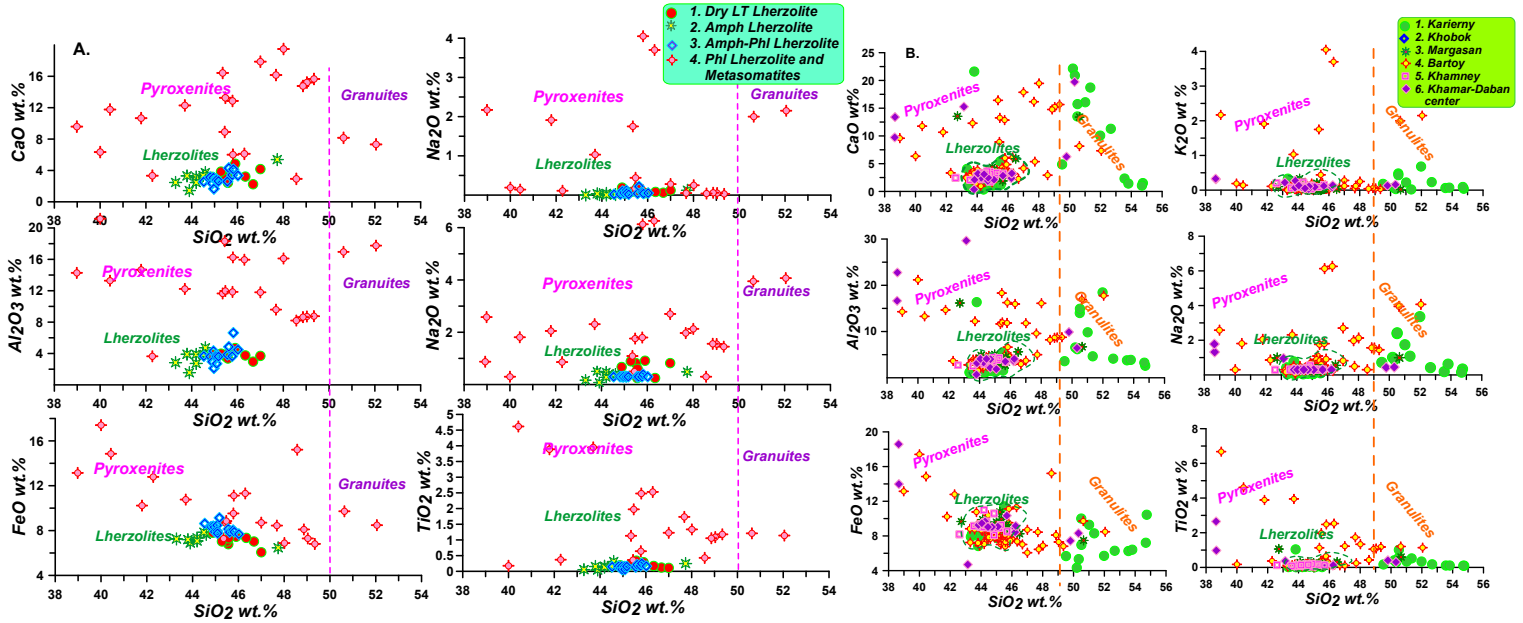

Angaro –Vitim Basolith in the late Paleozoic granitoid province of Western Transbaikalia (Fig. 2), better known as the Angara-Vitim batholith (Litvinovsky et al., 2011; Tsygankov, 2014; Tsygankov and Burmakina, 2026; Yarmolyuk et al., 1997), is one of the few areas on Earth where granitoids of different compositions were formed simultaneously over several tens of millions of years (Chen and Jahn, 2004; Eyal et al., 2010; Han et al., 1997; Whalen et al., 2006; Yarmolyuk et al., 2002; Zhao et al., 2008). Based on numerous single bond U - Pb determinations of the isotopic age of zircons from various types of granitoids in this province (more than 100 determinations), it has been established that granitoid magmatism took place in the period from approximately 325 to 280 Ma (Tsygankov and Burmakina, 2026).

In this article we are comparing the compositions and ages of the granulite xenoliths from the Cenozoic volcanics from Vitim Tunka and Bartoy volcanics to solve the question about their connections.

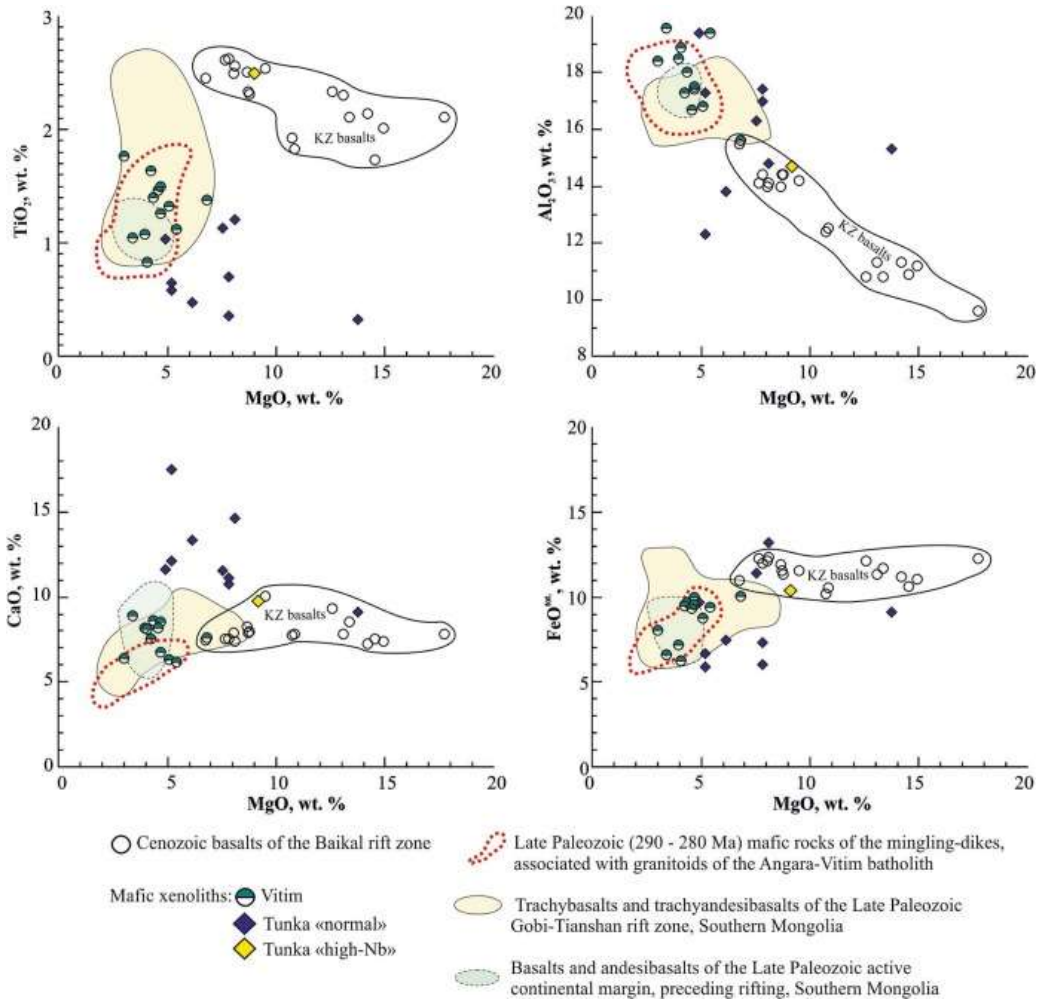

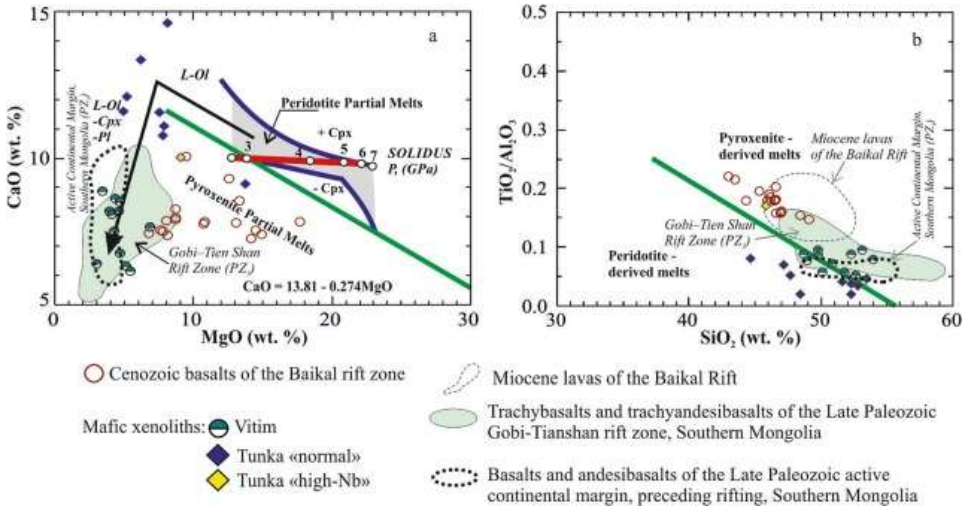

Fig.4. Position of the crustal mafic xenoliths and the host late Cenozoic basalts of the Baikal rift zone compositions (West Transbaikal and South Baikal volcanic areas) on the diagram CaO - MgO in primary magmas of fertile peridotite formed as a result of fractional melting. The blue lines define the upper and lower limits of CaO in these primary magmas (Herzberg and Asimov, 2008). In Fig. (a), lavas with CaO content lower than indicated by the green line are potential partial pyroxenite melts. The black broken arrow is the typical liquid line of descent for primary magmas that crystallize gabbro in the Earth's crust. The compositions of the Miocene lavas of the Baikal rift zone are shown for comparison (Demonterova et al., 2023), trachybasalts and trachyandesite basalts of the Late Paleozoic Gobi-Tianshan rift zone (Kozlovsky et al., 2006) and basalts and andesite basalts of the Late Paleozoic active continental margin, preceding rifting of the Southern Mongolia (Kozlovsky et al., 2006).

Fig. 5. Images of zircons from xenoliths

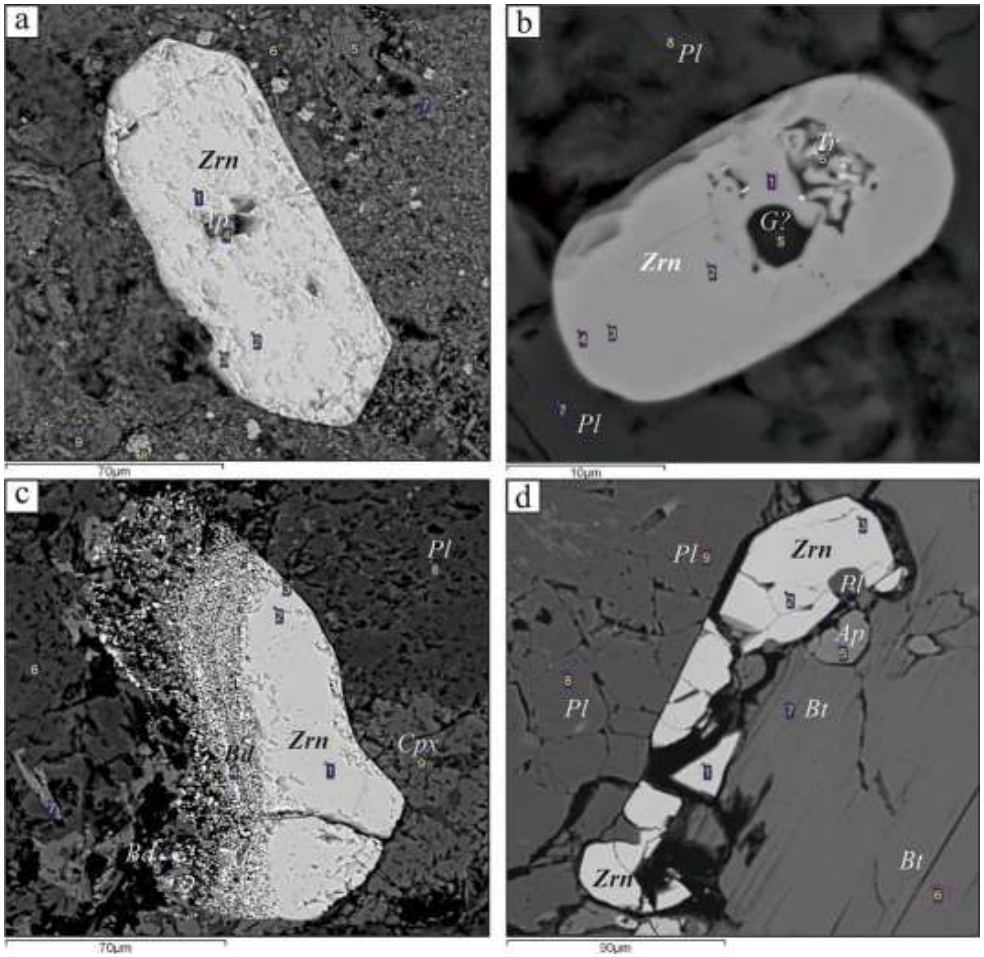

Fig. 6. Resalts of zircons from xenoliths dating. a –Tunka Karierny ; b- Vitim

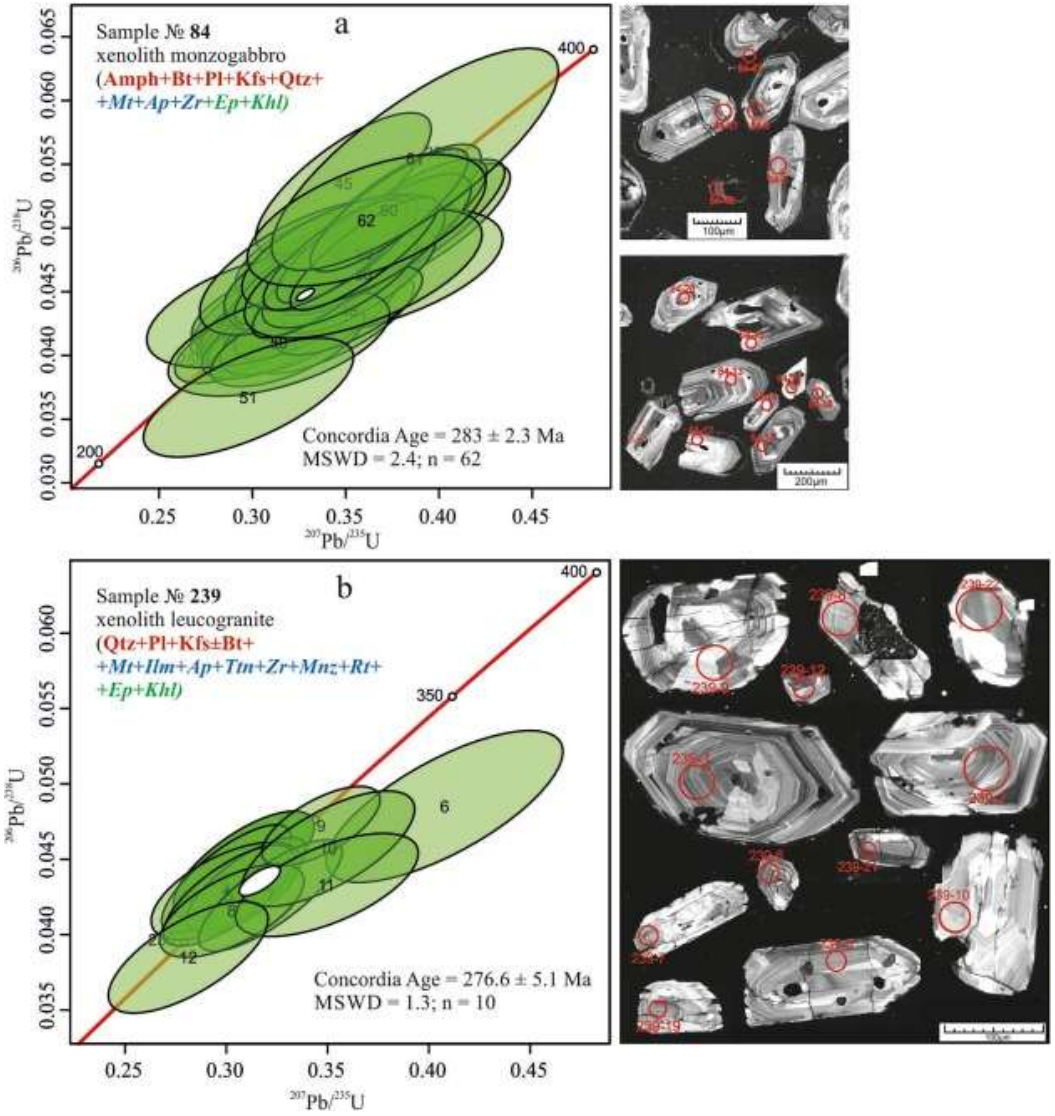

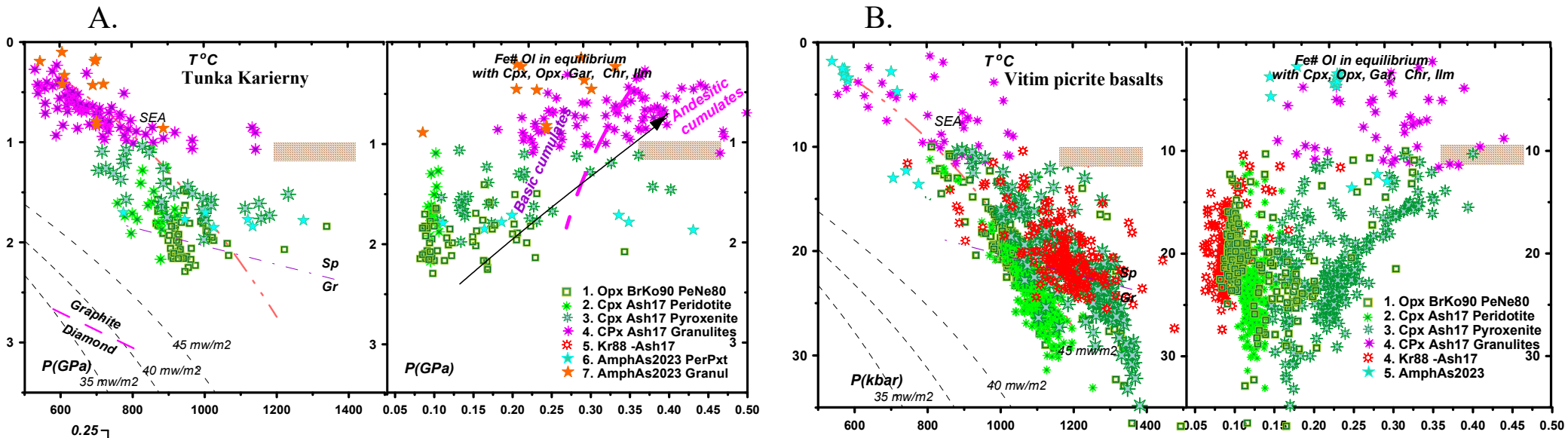

Fig. 7 A. PTX diagrams for the xenoliths and xenocrysts from Karirny volcano in Tunka valley and B. -Vitim picrite basalts.

Signs: 1. Opx: TºC (Brey and Kohler, 1990)-P(GPa)(McGregor, 1974). 2. Clinopyroxene Peridotite: TºC- (Nimis and Taylor, 2000) P(GPa) - Ashchepkov et al., 2017(Cr -diopsides); 3. Clinopyroxene Pyroxenite TºC (Nimis and Taylor, 2000 modified)–P(GPa) (Ashchepkov et al., 2017Un) for pyroxenites. 4. The same for granulites ; 5. Garnet (monomineral) 6..TºC (Krough, 1988) -P(GPa) (Ashchepkov et al., 2017), 5. Amphibole: TºC –P Ravna , 2000–P (GPa) corrected. The horizontal dashed line at 3.5 and 4.5 GPa corresponds to the Graphite-Diamond boundary at 35 and 40 mWm-2 respectively. Conductive geothems after (Pollack and Chapman), 1977

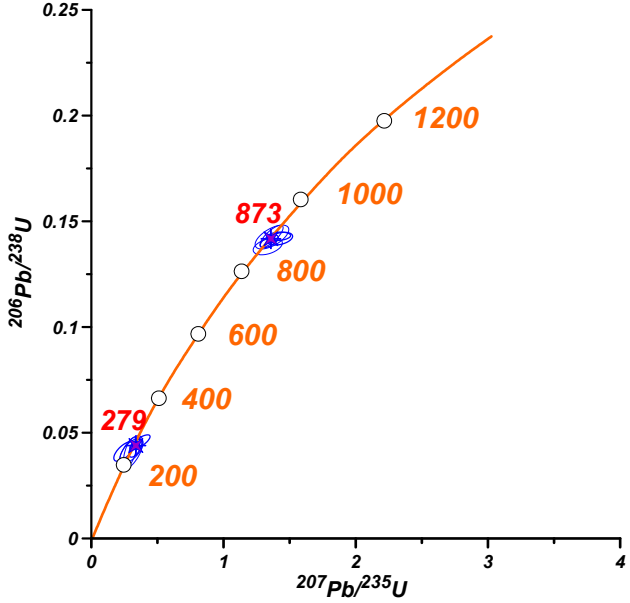

Fig.8 Ages of zircons from granulitic xenoliths from Vitim picrobasalts.

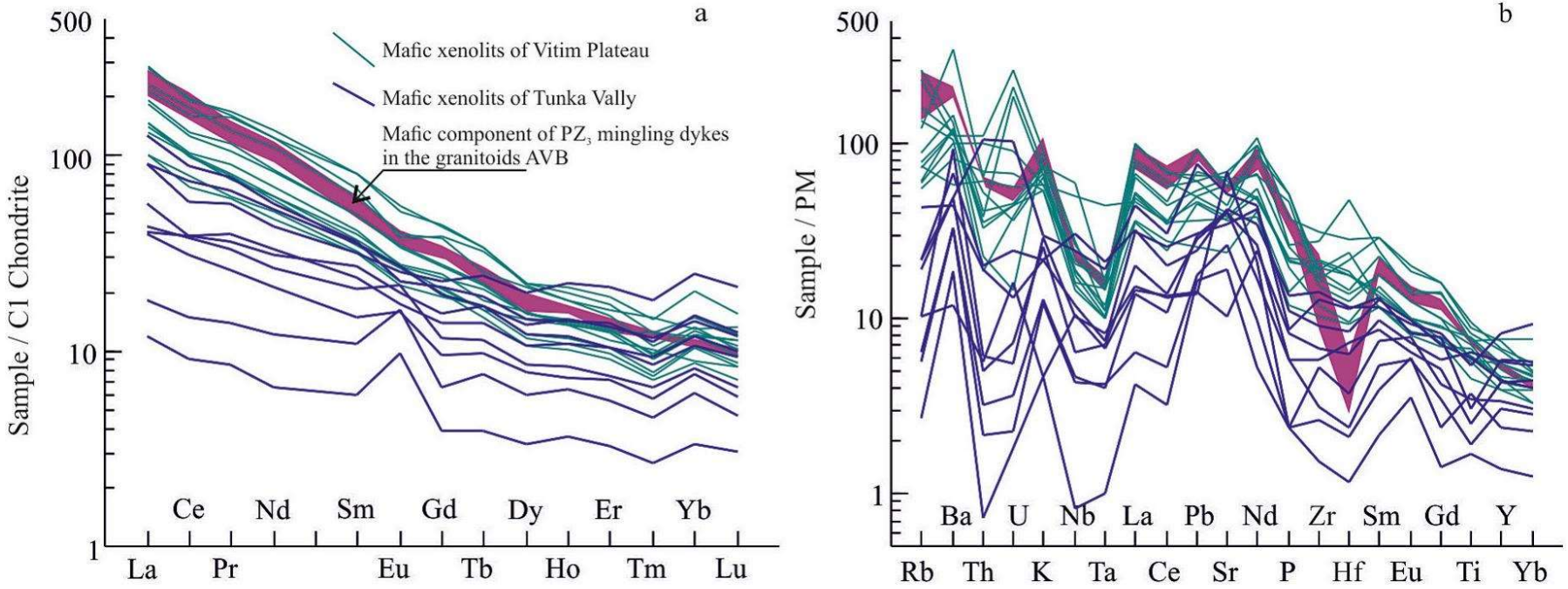

Fig.9. The trace-elements in the composition of mafic xenoliths from the Cenozoic basalts of the Baikal rift zone are compared to the mafic component of the mingling dyke of the Zhirim area (Burmakina et al., 2018) associated with the AVB granitoids. Figure (a) is normalized for C1 chondrite (Sun and McDonough, 1989); figure (b) is for primitive mantle (Palme and O'Neill, 2003).

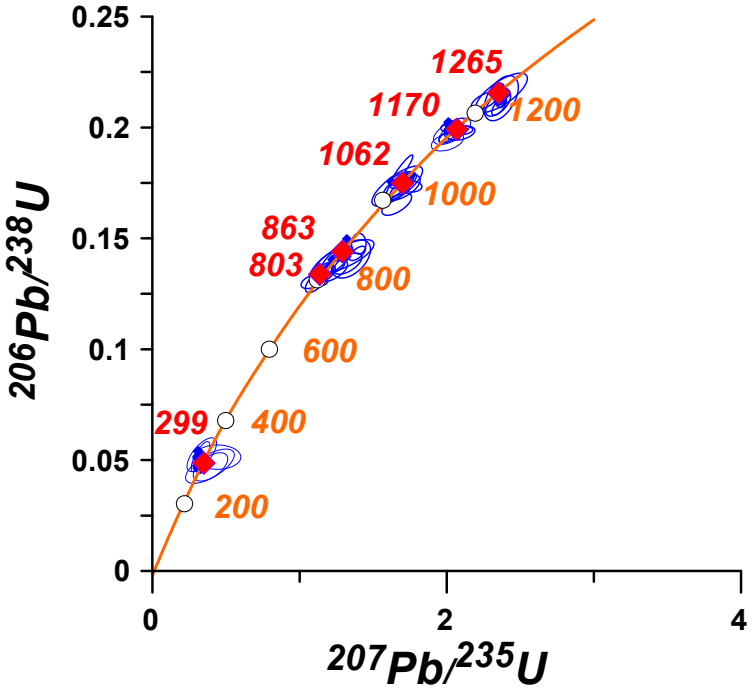

Fig. 10. Ages determined for the zircons from tuffs of Bartoy volcanoes.

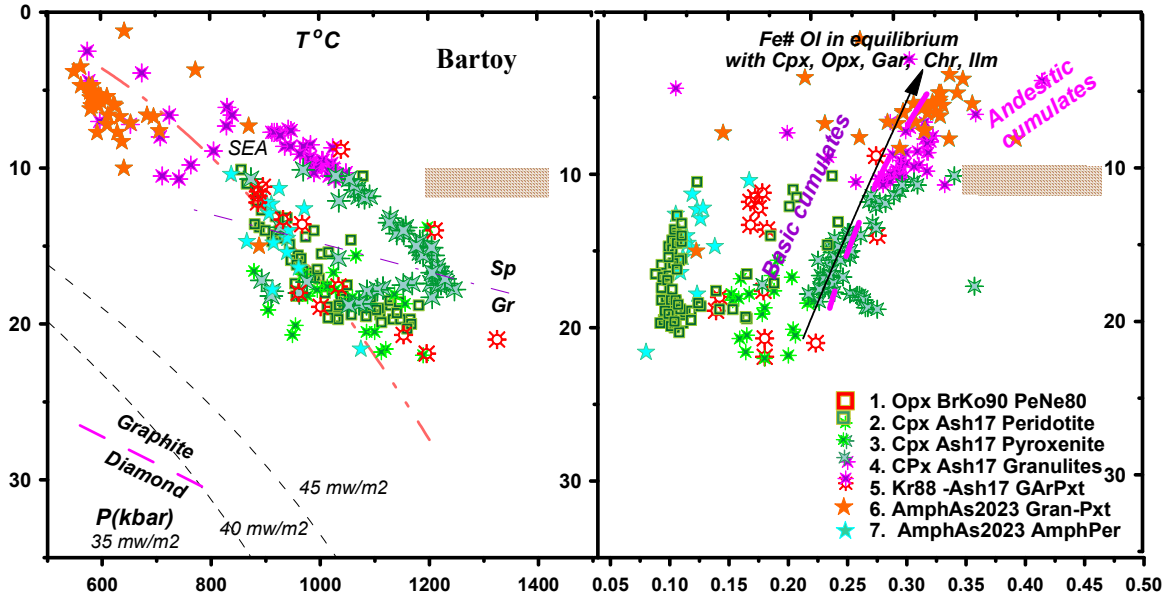

Fig. 11. . PTX diagrams for the xenoliths and xenocrysts from Bartoy volcanoes.

The ages of the zircons from tuffs 1150–1250 Ma mainly correspond to the meta-terrigenous rocks of the Shubutuiskaya Formation in the Khamar Daban zone. the Th/U ratio The Th/U ratio of 0.8–0.6 of these zircons
corresponds to the common magmatic rocks, mainly of the basic type. Dated granites in the Slyudyanka complex have ages of 470–515 Ma. Commonly the Khamar-Daban and Dzhida terrains are referring to the microplates. And the later terrain is thrusted over the Khamar-Daban. The collision events at the boundaries of the Paleoasian ocean occurred in the Vend-Cambrian and appeared mainly in Dzhida zone. The Neoproterozoic ages which we detected here 810–870 Ma were detected everywhere within the TKHVZ and these events corresponds to the volcanic and collision processes accompanied by the metamorphism. Though some plutons with the model ages 1100–800 Ma Igor et al. Earth Systems, Resources, and Sustainability, 2026, 1(2), 201–219 were suggested by some authors to be referred to the collision events. And elevated Th/U ratios of two zircons,
1.6–1.1, commonly correspond to the granites with the admixture of material of island arc environment with 3–5 Th/U ratios. More ancient 1170–1265 Ma are more typical for the Khamar-Daban for Gar-Biotite shists and
gneisses of Kornilovskaya formation then for southern border where we found them. And this probably suggest the deeper zones of the crust is Dzhida may be also similar to the Centrakl Khamar Daban and collision complexes are over-thrusted. The age of granitic zircon, 300 Ma, just corresponds to the beginning of the Angaro-Vitim Batholith formation. It may be connected to the movement of the superplume-formed kimberlites in Yakutia at the interval 420–340 Ma and later created the Biryusa and Tumanshet lamproites and later the Ingashi lamproites in Eastern Sayan ~306–309 Ma. Further movement through Khamar-Daban and interaction with the lower crust and granulites brings to the creation of alkaline granitoids of AVP. But the Th/U ratio is rather low, 0.07, which commonly corresponds to the metamorphic type [89]; thus, they should be from granulites possibly remelted by a plume. Over time, volcanism manifested first in the center of the TKHVZ zone and then gradually spread to the south and north, forming volcanoes of the central type in the rift basins.

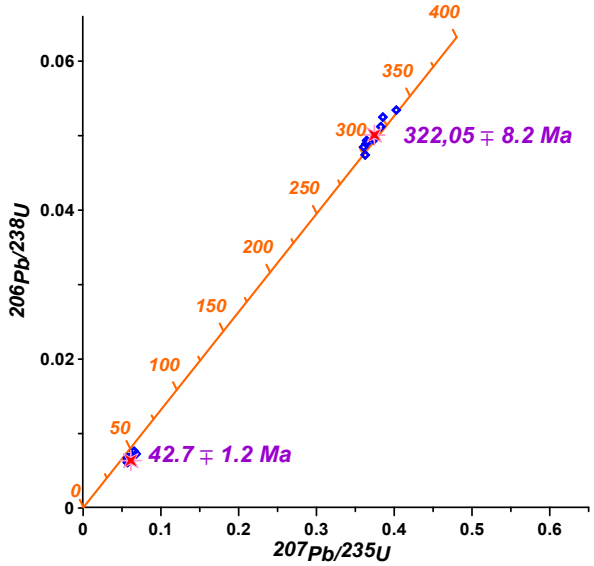

Fig. 12. Ages determined for zircons from granulitic xenoliths from Shavaryn-Tsaram volcano. The stars are the average ages for xenolith Shav22-24 and Shav19-24.

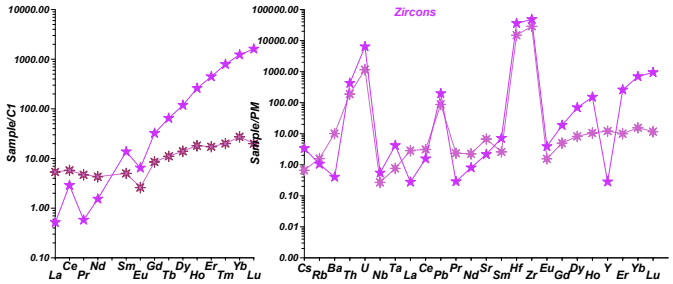

Fig.13 REE and TRE diagrams for zircons from Shav22-24 and Shav19-24 xenoliths.

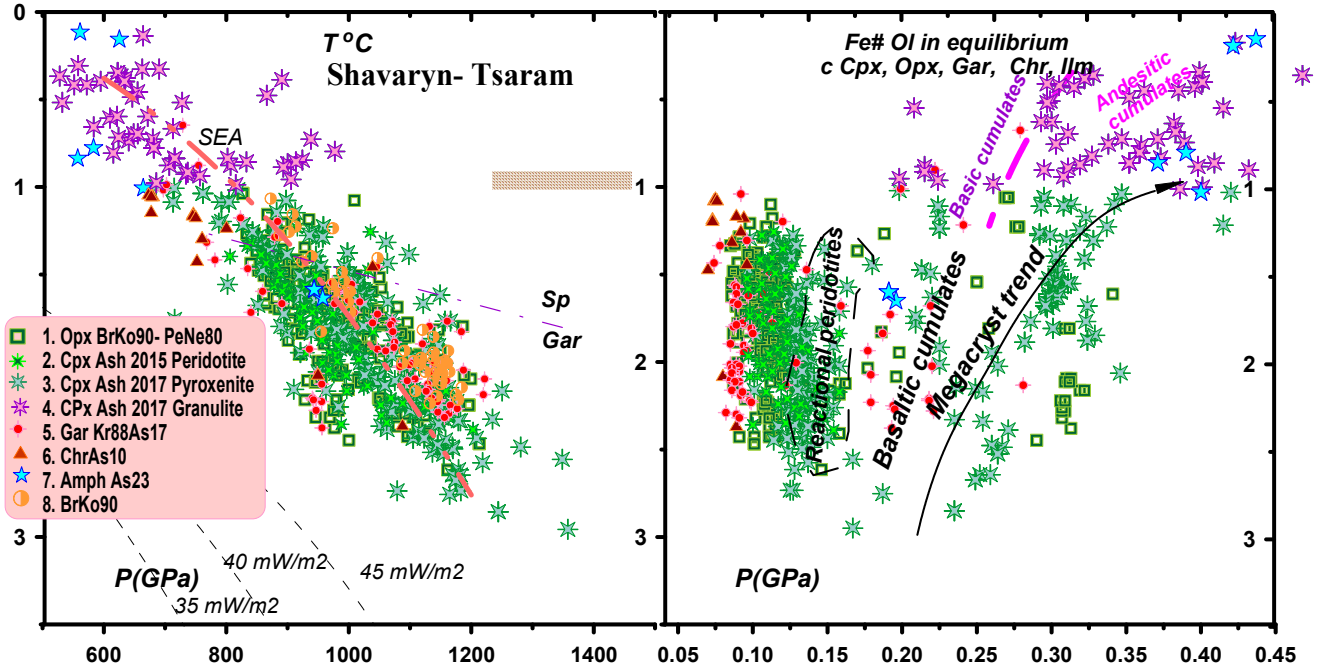

Fig. 14. PTX diagrams for the xenoliths and xenocrysts from Shavaryn -Tsram volcano, Mongolia.

The dating of zircons displays the Carboniferous stage of rifting in Mongolia (Kozlovsky et al., 2005) some authors suggest the slab window model (Zhou et al., 2021) which is similar to the plume magmatism. It is close to the initial stage of Angaro-Vitim batholith formation.Further study and dating of the crust xenoliths and xenocrysts could allow compiling the detail models of the mantle and crust magmas generation and joint evolution of the mantle Moho and crust in the Transbaikalia. So it is necessary to conclude that the basic plume magmatism is strongly affecting on the crust material producing acid magmas and bi-modal series.

Ashchepkov, I.V. Deep xenoliths of the Baikal rift. Novosibirsk: Nauka, Siberian Branch, 1991. 160 p.

Ashchepkov, I.V., Ntaflos, T., Logvinova, A.M., Spetsius, Z.V., Downes, H., Vladykin, N.V. Monomineral universal clinopyroxene and garnet barometers for peridotitic, eclogitic and basaltic systems. Geoscience Frontiers. 2017. No. 8, 775–795. DOI: 10.1016/j.gsf.2016.06.012

Ashchepkov, I. V., Travin, S. V., Saprykin, A. I., Andre, L., Gerasimov, P. A., Khmel'nikova, O. S. 2003. Age of xenolith-bearing basalts and mantle evolution in the Baikal rift zone. Russian Geology and Geophysics, 44(11), 1160-1188.

Ashchepkov, I.V., Andre, L., Downes, H., Belyatsky, B.A. 2011. Pyroxenites and megacrysts from Vitim picrite-basalts (Russia): Polybaric fractionation of rising melts in the mantle? Journal of Asian Earth Sciences, 42(1-2), 14-37.

Ashchepkov I.V., Tsygankov A.A., Burmakina G.N., Karmanov N.S., Rasskazov S.V., Chuvashova I.S., Ailow Y. Thermal state and nature of the lower crust in the Baikal Rift Zone: Insight from xenoliths of Cenozoic and Paleozoic magmatic rocks // Geosystems and Geoenvironment, 2024, 100305, DOI: 10.1016/j.geogeo.2024.100305

Ashchepkov, I., Tsygankov, A., Burmakina, G., Ntaflos, T., Rasskazov, S., Chuvashova, I., Ailow, Y. (2026). Geochemistry and Petrology of Crust and Mantle Xenoliths and Xenocrysts in the Trans-Khamar-Daban Zone. Earth Systems, Resources, and Sustainability, 1(2), 202-220.

Ashchepkov, I. V., Tsygankov, A. A., Burmakina, G. N. (2025). Peridotite pyroxenite and granulite xenoliths from Cenozoic Shavaryn Tsaram volcanic center (Mongolia): New data. Geosystems and Geoenvironment, 100484.

Tsygankov, A. A., Burmakina, G. N., Ashchepkov, I. V. (2026). Lower crust of the Baikal rift zone (Transbaikalia, Russia): Testing a model of late Paleozoic mafic underplating. Lithos, 108519.

Tsygankov A.A., Khubanov V.B., Burmakina G.N., Elbaev A.L., Burdukovsky V.V., 2019. Correlation between the mantle and heterochronous crustal materials in the composition of Transbaikalia A-type granitoides: petrological and geodynamical implications. Geodynamics & Tectonophysics 10 (3), 779–799.

Tsygankov, A.A., 2014. Late Paleozoic granitoids in western Transbaikalia: sequence of formation, sources of magmas, and geodynamics. Russ. Geol. Geophys. 55, 153–176.

Tsygankov, A.A., Burmakina, G.N., Khubanov, V.B., Buyantuev, M.D., 2017. Geodynamics of late Paleozoic Batholith-Forming processes in Western Transbaikalia. Petrology 25, 396–418.

Tsygankov, A.A., Khubanov, V.B., Udoratina, O.V., Coble, M.A., Burmakina, G.N., 2021. Alkaline granitic magmatism of the Western Transbaikalia: Petrogenetic and geodynamic implications from U-Pb isotopic–geochronological data. Lithos. 390-391. 106098.

Tsygankov, A.A., Litvinovsky, B.A., Jahn, B.M., Reichow, M.K., Liu, D.Y., Larionov, A.N., Presnyakov, S.L., Lepekhina, Ye, Sergeev, S.A., 2010. Complex sequence of magmatic events in the Late Palaeozoic of Transbaikalia, Russia (U–Pb isotope data). Russian Geology and Geophysics 51, 901–922.

Tsygankov, A.A., Matukov, D.I., Berezhnaya, N.G., Larionov, A.N., Posokhov, V.F., Tsyrenov, B.Ts., Khromov, A.A., Sergeev, S.A., 2007b. Late Paleozoic granitoids of western Transbaikalia: magma sources and stages of formation. Russian Geology and Geophysics 1, 156–180.

Acknowledgements

Work is the supported by the Ministry of Science and Higher Education of the Russian Federation and Russian Science Foundation and partially by Russian Science Foundation (20-27-00030).

Work was done on state assignments of Dobretsov NL Geological institute and Sobolev VS IGM SB RAS. The authors would like to thank the staff of the analytical services of GI and IGM SB RAS.

Thank you for attention !